Thermoresponsive Polymer Micelles as Potential Nanosized Cancerostatics

ARTICLE *in* BIOMACROMOLECULES · JULY 2015

Impact Factor: 5.75 · DOI: 10.1021/acs.biomac.5b00764 · Source: PubMed

8 AUTHORS, INCLUDING:

Olga Janouskova

Academy of Sciences of the Czech Republic

26 PUBLICATIONS **93** CITATIONS

SEE PROFILE

Karel Ulbrich

Academy of Sciences of the Czech Republic

319 PUBLICATIONS **11,293** CITATIONS

SEE PROFILE

Tomas Etrych

Academy of Sciences of the Czech Republic

64 PUBLICATIONS **2,175** CITATIONS

SEE PROFILE

Michal Pechar

Academy of Sciences of the Czech Republic

49 PUBLICATIONS **1,027** CITATIONS

SEE PROFILE

Article

pubs.acs.org/Biomac

Thermoresponsive Polymer Micelles as Potential Nanosized Cancerostatics

Richard Laga,* Olga Janoušková, Karel Ulbrich, Robert Pola, Jana Blažková, Sergey K. Filippov, Tomáš Etrych, and Michal Pechar

Institute of Macromolecular Chemistry, Academy of Sciences of the Czech Republic, v.v.i, Department of Biomedical Polymers, Heyrovský square 2, 162 06 Prague, Czech Republic

Supporting Information

ABSTRACT: An effective chemotherapy for neoplastic diseases requires the use of drugs that can reach the site of action at a therapeutically efficacious concentration and maintain it at a constant level over a sufficient period of time with minimal side effects. Currently, conjugates of high-molecular-weight hydrophilic polymers or biocompatible nanoparticles with stimuli-releasable anticancer drugs are considered to be some of the most promising systems capable of fulfilling these criteria. In this work, conjugates of thermoresponsive diblock copolymers with the covalently bound cancerostatic drug pirarubicin (PIR) were synthesized as a reversible micelle-forming drug delivery system combining the benefits of the above-mentioned carriers. The diblock copolymer carriers were composed of hydrophilic poly[*N*-(2-hydroxypropyl)methacrylamide]-based block containing a small amount (~5 mol %) of comonomer units with reactive hydrazide groups and a thermoresponsive poly[2-(2-methoxyethoxy)ethyl methacrylate] block. PIR was attached to the hydrophilic block of the copolymer through the pH-sensitive hydrazone bond designed to be stable in the bloodstream at pH 7.4 but to be degraded in an intratumoral/intracellular environment at pH 5−6. The temperature-induced conformation change of the thermoresponsive block (coil−globule transition), followed by self-assembly of the copolymer into a micellar structure, was controlled by the thermoresponsive block length and PIR content. The cytotoxicity and intracellular transport of the conjugates as well as the release of PIR from the conjugates inside the cells, followed by its accumulation in the cell nuclei, were evaluated in vitro using human colon adenocarcinoma (DLD-1) cell lines. It was demonstrated that the studied conjugates have a great potential to become efficacious in vivo pharmaceuticals.

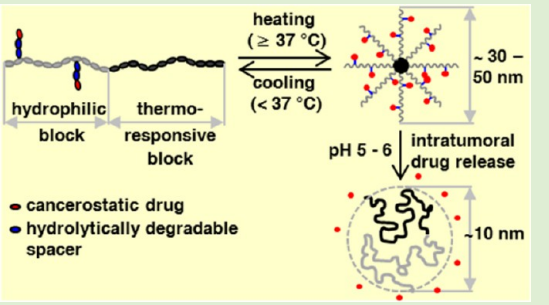

INTRODUCTION

Currently, neoplastic diseases, together with cardiovascular diseases, two of the most common fatal illnesses, represent a serious health problem in patient populations.[1] The treatment of neoplastic diseases using conventional chemotherapeutics—low-molecular-weight compounds with cancerostatic effects—may lead to the suppression or even a complete cure of the disease; however, such treatment is usually associated with particular side effects. These side effects are mainly the result of ineffective localization of a cytotoxic drug in a tumor, often leading to irreversible damage to healthy cells and tissue. Moreover, the treatment using low-molecular-weight chemotherapeutics commonly requires relatively frequent dosing, as the drug concentration at the site of action rapidly decreases due to rapid blood clearance, glomerular filtration, and drug elimination.

The chemotherapeutic strategy using conjugates of high-molecular-weight (HMW) synthetic hydrophilic polymer carriers with covalently linked drugs is considered to be one of the most effective ways to prolong blood clearance and reliably reduce unwanted side effects.[2] Based on the differences in the endothelial permeability of the healthy and the malignant tissues, such conjugates are able to deliver the drug preferentially to the tumor tissue without significantly affecting the healthy cells.[3−5] Furthermore, a properly chosen stimuli-sensitive biodegradable linker inserted between the polymer backbone and the drug may ensure the conjugate stability in the circulation and a long-lasting release of the drug directly inside the tumor or the cancer cells.[6−8]

It was shown that the level of the passive accumulation of the conjugates in the solid tumors due to the enhanced permeability and retention (EPR) effect depends to a large extent on the size or molecular weight of the polymer carrier.[9] Current synthetic procedures enable the preparation of polymer-drug conjugates with a broad range of molecular weights and sizes of polymer coils.[10,11] Unfortunately, the elimination of such conjugates from the body after delivering the drug (one of the basic requirements for drug delivery carriers) is limited by the molecular weight, e.g., for *N*-(2-hydroxypropyl)methacrylamide (HPMA)-based polymers not exceeding 50 kDa, unless they are biodegradable.[9] The size of such macromolecules is rather small to achieve an efficient EPR

Received: June 8, 2015
Revised: July 3, 2015

DOI: 10.1021/acs.biomac.5b00764
Biomacromolecules XXXX, XXX, XXX−XXX

effect and the synthesis of biodegradable HMW conjugates is not a simple task. HMW drug carriers based on polymer micelles prepared by self-assembly of smaller amphiphilic copolymers (excretable in a form of unimer) offer a beneficial solution to this problem. Such nanosized materials are usually prepared from block or graft copolymers consisting of hydrophilic and hydrophobic chains of various lengths and compositions. Copolymers based on nonreactive poly(ethylene glycol)/poly(L-lactide), poly(ethylene glycol)/poly(γ-benzyl-L-glutamate) or poly(ethylene glycol)/poly(propylene glycol) are among the most examined ones.[12−14] These copolymers have been described as carriers of hydrophobic drugs which, in most cases, were noncovalently (hydrophobic interaction) incorporated into the hydrophobic core of the micelles through the self-assembly process. In spite of the structural and morphological variability of these materials, the relatively difficult preparation of the defined micelles, together with their tendency to aggregate, lower drug loading, and complicated long-term storage, limits their clinical application.

A suitable alternative to the above-mentioned polymer micelles might be reversible temperature-sensitive micelles comprising a combination of hydrophilic and thermoresponsive block copolymers. The thermoresponsive polymers are distinct in their ability to reversibly change the chain morphology—from the random coil conformation (soluble form), to the condensed globule (insoluble form)—depending on the temperature of the incubation media. From the biomedical application point of view, the coil−globule transition temperature (T_{tr}) of the thermoresponsive polymer chain should be slightly below physiological temperature (37 °C) to allow for the easy dissolution of the block copolymer in laboratory conditions and spontaneous formation of the defined micelles immediately before (by heating up the solution to 37 °C) or upon sample administration. Copolymers based on poly(*N*-isopropylacrylamide) (poly(NIPAAm)),[15,16] poly(2-isopropyl-2-oxazoline) (poly(IPOX))[17,18] and elastin side-chain polymers[19] are examples of the most commonly studied materials meeting these requirements, although the individual polymers exhibit particular pitfalls that might prevent their possible application in the clinics. These limitations are the relatively strong dependence of the T_{tr} on the degree of polymerization (poly(NIPAAm)), the concentration (elastin-based polymers), and the relatively complex preparation technique that does not allow the synthesis of HMW uniform polymers (poly(IPOX)).[20,21]

Considering the facts mentioned above, copolymers based on the poly[2-(2-methoxyethoxy)ethyl methacrylate] (poly(DEGMA)) seemed to be suitable candidates for the proposed purposes as they fully meet the criteria for the biomedical application including the nontoxicity, biocompatibility, and transition temperature requirements ($T_{tr} \approx 24-28$ °C) and do not show the limitations observed in the case of the above-mentioned materials.[20,22,23] In this study, we used the unique combination of thermoresponsive poly(DEGMA) with the highly hydrophilic *N*-(2-hydroxypropyl)methacrylamide copolymers (poly(HPMA)), which have often been applied as carriers for drug, protein or gene delivery.[24−26] The initial diblock copolymer precursors with various lengths of the thermoresponsive poly(DEGMA) blocks were synthesized by the reversible addition−fragmentation chain-transfer (RAFT) polymerization technique, enabling the preparation of the precisely defined materials. The poly(HPMA) block contained ∼5 mol % of comonomer units with hydrazide groups intended for the attachment of the cancerostatic drug pirarubicin (PIR). PIR was bound to the hydrophilic blocks of the copolymers through the pH-sensitive hydrazone bond, which proved to be stable in the bloodstream at pH 7.4 but to undergo pH-sensitive hydrolysis in the intratumoral and intracellular environment at pH below 6.5. The influence of the physicochemical parameters of the conjugates on their in vitro biological behavior was investigated using the colorectal adenocarcinoma DLD-1 cell lines. It was demonstrated that the studied conjugates effectively penetrated the cell membranes of the cancer cells and released PIR inside the cells, which resulted in changed cell morphology and damaged mutual intracellular connections, both indicating approaching cell death.

EXPERIMENTAL SECTION

Materials. (*RS*)-1-Aminopropan-2-ol, 6-aminohexanoic acid (Ahx), 2,2′-azobis(2-methylpropionitrile) (AIBN), 2-cyano-2-propyl benzodithioate (CPB), 4-cyano-4-thiobenzoylsulfanylpentanoic acid (CTP), *N*,*N*′-dicyclohexylcarbodiimide (DCC), *N*,*N*′-dimethylacetamide (DMA), dimethyl sulfoxide (DMSO), 1,4-dioxan, methacryloyl chloride, 2-(2-methoxyethoxy)ethyl methacrylate (DEGMA), *tert*-butanol, *tert*-butyl carbazate, triisopropylsilane (TIPS), trifluoroacetic acid (TFA), and 2,4,6-trinitrobenzenesulfonic acid solution (1 M in H2O) were purchased from Sigma-Aldrich (Sigma-Aldrich spol. s r.o., Czech Republic). PIR was obtained from Meiji Seika Pharma Co., Ltd. (Japan), and DY-676 NHS-ester was purchased from Dyomics GmbH (Germany). All other chemicals and solvents were of analytical grade. Solvents were dried and purified by conventional procedures and distilled before use.

The EL-4 and DLD-1 cell lines were obtained from ATCC (LGC Standards Sp. z o.o., Poland). Dulbecco's Modified Eagle Medium (DMEM) and RPMI-1640 media, Alamar Blue cell viability reagent and Hoechst 33342 were purchased from Life Technology (Life Technologies Czech Republic s.r.o., Czech Republic).

Size-Exclusion Chromatography (SEC). The molecular weights and polydispersities of the polymers and polymer-PIR conjugates were determined by SEC on a Shimadzu HPLC system equipped with UV−VIS diode array detector (Shimadzu, Japan), refractive index Optilab-rEX, and multiangle light scattering DAWN EOS detectors (Wyatt Technology Corp., Santa Barbara, CA). TSK-Gel SuperAW3000 and SuperAW4000 columns connected in series and 80% methanol/20% sodium acetate buffer (0.3 M, pH 6.5) as an eluent at a flow rate of 0.6 mL/min were used in all experiments. A method based on the known total injected mass with an assumption of 100% recovery was used for the calculation of the molecular weights from light scattering data. The number- and weight-average molecular weights for the polymer precursors and the polymer−PIR conjugates are summarized in Table 1 and Table 2, respectively.

UV/Vis Spectrophotometry. The spectrophotometric analyses were carried out in quartz glass cuvettes on a UV/vis spectrophotometer Helios Alpha (Thermospectronic, UK). The content of dithiobenzoate (DTB) end groups in the polymers were determined at 302 nm in methanol using the molar absorption coefficient ε^{DTB} = 12 100 L/mol·cm. The content of hydrazide groups in the polymer precursors was determined using a modified TNBSA assay as described earlier.[27] The results are summarized in Table 1. The determination of the PIR content in the polymer−PIR conjugates (without fluorophore) was performed at 488 nm in methanol using the molar absorption coefficient ε^{PIR} = 11 300 L/mol·cm. The PIR contents are summarized in Table 2. The content of carbonylthiazolidine-2-thione (TT) reactive groups in the polymer precursor was determined at 305 nm using the molar absorption coefficient ε^{TT} = 10 300 L/mol·cm.

Dynamic Light Scattering (DLS). The hydrodynamic radii (RH) and scattering intensities (IS) of the polymer precursors and polymer conjugates were measured by the DLS technique at a scattering angle θ = 173° using a Nano-ZS instrument (Model ZEN3600, Malvern Instruments, UK) equipped with a 632.8 nm laser. The temperature

DOI: 10.1021/acs.biomac.5b00764
Biomacromolecules XXXX, XXX, XXX−XXX

Table 1. Molecular Weight Parameters of the Copolymer Precursors PP1−PP4 Obtained from SEC Analysis

polymer precursor	structure	[PP1]/[DEGMA][a]	M_n[b] [g/mol]	$Đ$[c]	T_{tr} [°C]
PP1	p[(HPMA)-*co*-(Ma-Ahx-NHNH-Boc)]	-	14 100	1.11	-
PP2	p[(HPMA)-*co*-(Ma-Ahx-$NHNH_2$)]-*b*-p(DEGMA)	1/38	21 100	1.55	44
PP3	p[(HPMA)-*co*-(Ma-Ahx-$NHNH_2$)]-*b*-p(DEGMA)	1/76	31 000	1.47	33
PP4	p[(HPMA)-*co*-(Ma-Ahx-$NHNH_2$)]-*b*-p(DEGMA)	1/114	38 700	1.51	31

[a]Molar ratios of DTB-end groups of **PP1** precursor to DEGMA monomer in the polymerization feed. [b]Number-averaged molecular weights evaluated by GPC using the LS and RI detectors. [c]Polydispersity indexes (ratios of weight- and number-averaged molecular weights).

Table 2. Physicochemical Characteristics of the Thermoresponsive Polymer−PIR Conjugates PC2−PC4

polymer conjugate	PC2	PC3	PC4
polymer precursor	PP2	PP3	PP4
M_n[a] [g/mol]	21 500	31 800	40 000
$Đ$[b]	1.43	1.47	1.46
ω^{PIR}[c] [wt %]	7.9	7.3	7.3
D_H^{rcd} [nm] ($T < T_{tr}$)	8.4	8.9	10.6
D_H^{mice} [nm] ($T > T_{tr}$)	31.5	37.3	50.0
T_{tr} [°C]	39	30	26
CMC [mg/mL]	0.071	0.053	0.022

[a]Number-averaged molecular weights evaluated by SEC using a relative calibration. [b]Polydispersity indexes (ratios of weight- and number-averaged molecular weights). [c]Weight contents of PIR in polymer-PIR conjugates. [d]Hydrodynamic diameters of polymer-PIR conjugate particles (polymer micelles) below the transition temperature. [e]Hydrodynamic diameters of polymer-PIR conjugate particles (unimers) above the transition temperature.

measurements were performed to investigate the self-assembly of polymer coils to polymer micelles in the temperature range 20−50 °C (in 1 °C increments) in PBS (1.0 mg/mL, pH 7.4) solutions. At each step, measurements were performed after reaching the steady state conditions, which typically required approximately 10 min. For the evaluation of the dynamic light scattering data, the DTS(Nano) program was used. The mean of at least three independent measurements was calculated. The transition temperature (T_{tr}) characterizing the polymer chain conformation changes was evaluated from the temperature dependence of the hydrodynamic diameter (D_H); the T_{tr} value was determined from the intersection point of two lines formed by the linear regression of a lower horizontal asymptote and a vertical section of the S-shaped curve (sigmoidal curve) fit. The T_{tr} values for the polymer precursors and the polymer−PIR conjugates are summarized in Table 1 and Table 2, respectively.

PIR Release Assays. The release of PIR from the polymer−PIR conjugates was measured in aqueous solutions at 37 °C at two different pH values using a monochromator-based multimode microplate reader Synergy H1 (BioTek, USA). Specifically, the polymer conjugates (c = 2.5 mg/mL) were dissolved in 0.15 M PBS (pH 5.5 or 7.4), heated up to 37 °C, and kept at this temperature for the duration of the analysis. In the selected time intervals, the aliquots (140 μL) were loaded on the preheated PD SpinTrap G-25 columns (GE Healthcare, UK) and centrifuged at 37 °C for 2 min at 800 × g. Subsequently, the absorbances of the collected polymer fractions were measured in 96-well plates at 486 nm. The PIR release from the polymer−PIR conjugates was plotted as the relative decrease of amount of polymer-bound pirarubicin over time. An absorbance of the appropriate polymer−PIR conjugate measured immediately upon its dissolution and subsequent centrifugation was used as an initial value ($A(t_0)$).

The stabilities of the polymer−PIR conjugates in the buffers modeling both extracellular and intracellular environments were also evaluated using a SEC column on the Shimadzu HPLC system (see above). Specifically, the polymer conjugates (c = 1.0 mg/mL) were dissolved in 0.15 M PBS (pH 5.5 or 7.4), heated up to 37 °C and kept at this temperature for the duration of the analysis. At selected time intervals, the aliquots (20 μL) were loaded on the TSK-Gel SuperAW3000/4000 column and eluted using the 80% methanol/20% sodium acetate buffer (0.3 M, pH 6.5) mixture. The relative amount of the polymer-bound PIR was evaluated from the polymer peak area recorded by the UV−VIS detector at 486 nm. The release of PIR from the conjugates was plotted as a change of the polymer-bound PIR concentration over time.

Isothermal Titration Calorimetry (ITC). The critical micellar concentration (CMC) values were determined by an isothermal titration microcalorimeter MicroCal *i*TC200. The ITC experiments were performed using either 20 injections of the polymer solution in PBS buffer above the T_{tr} into PBS buffer (a constant titration volume of 2 μL; 180 s intervals). The thermograms were recorded and analyzed using Origin 7 software.

Cell Line Cultures. EL-4 murine T-cell lymphoma cell line was cultured in DMEM supplemented with heat inactivated 10% fetal calf serum (FCS), penicillin (100 U/mL), and streptomycin (100 μg/mL). The DLD-1 human colorectal adenocarcinoma cell line was cultured in RPMI-1640 medium with heat inactivated 10% FCS, penicillin (100 μg/mL), and streptomycin (100 μg/mL).

In Vitro Cell Viability Assay. DLD-1 (5 × 104) or EL4 cells (15 × 104) were seeded in 100 μL media into 96-well flat-bottom plates 24 h before the addition of the polymer−PIR conjugates or free PIR. The polymer−PIR conjugate stock solutions (5 mg/mL in PBS) were diluted with PBS to concentrations ranging from 0.2 to 200 μg/mL; PIR was first dissolved in DMSO (10 mg/mL) and then diluted with PBS to 0.01−100 μg/mL. Thereafter, 10 μL of the polymer−PIR conjugates or PIR were added to the cells and the cells were cultured for 72 h in 5% CO_2 atmosphere at 37 °C. Then, 10 μL of Alamar Blue cell viability reagent was added to each well and allowed to incubate for 4 h at 37 °C. In viable cells, the active component of the Alamar Blue reagent—resazurin—was reduced to the highly fluorescent compound resorufin. The fluorescence of resorufin was detected using the Synergy Neo plate reader (BioTek, USA) at 570/610 nm (excitation/emission). The cells cultured in a medium without Alamar Blue were used as negative controls. Three wells were used for each concentration. The assay was repeated three times independently. Statistical analysis for one-way ANOVA was performed using the GraphPad Prism Software. The IC_{50} values for the polymer−PIR conjugates and free PIR are summarized in Table 3.

Internalization of Fluorescently Labeled Polymer−PIR Conjugates. DLD-1 cells were cultured for 24 h in 5% CO_2 atmosphere at 37 °C on a 35 mm glass bottom dish with four chambers, a 20 mm microwell, and a #1 cover glass (0.13−0.16 mm). The amount of the fluorescently labeled polymer−PIR conjugate added to the cell suspensions was normalized to the DY-676 content (1 μg DY-676/mL), corresponding to the final conjugate concentration of 100 μg/mL. After 2, 4, 8, 16, 24, and 48 h, the native cells were washed three times with PBS, and the nuclei were with 5 μg/mL of Hoechst 33342. DY-676-labeled polymer conjugates were excited at 674 nm, and the emitted light was detected at 699 nm. PIR was excited at 488 nm and the emission was measured through a 500−600 nm filter. Hoechst 33342 dye was excited at 405 nm and the emitted light was measured through a 450−500 nm filter. The fluorescence and transmitted light was acquired using a laser scanning confocal microscope (LSCM) Olympus IX83 with the FV10-ASW software (Olympus, Czech Republic). The samples were scanned with a 60 × oil immersion objective Plan ApoN (1.42 numerical aperture; Olympus, Czech Republic).

DOI: 10.1021/acs.biomac.5b00764
Biomacromolecules XXXX, XXX, XXX−XXX

Table 3. IC_{50} Values for the Polymer−PIR Conjugates and Free PIR Measured on DLD-1 and EL-4 Cell Lines Using the Cell Viability Assay

	IC_{50} [μg/mL]	
Sample	DLD-1	EL-4
PC2	3.26	0.0118
PC3	2.92	0.0153
PC4	3.11	0.0120
PIR	0.16	>0.0001
PC5[a]	1.41	0.0004
PC6	16.45	n.d.

[a]Conjugate of hydrophilic p[(HPMA)-*co*-(Ma-Ahx-$NHNH_2$)] polymer precursor with PIR bound to the polymer backbone through the hydrolytically degradable hydrazone bond (M_w = 36 800 g/mol, M_w/M_n = 1.92, ω^{PIR} = 8.9 wt %) prepared as described.[36] For the structure, see Figure S1A.

Competitive Hoechst Staining - Detection of Doxorubicin in Cell Nuclei. DLD-1 cells were incubated with free PIR or with the polymer−PIR conjugates at concentration 100−0.01 μg/mL of PIR under standard culture conditions. After 24 h, the cells were detached with a detaching solution (100 mM HEPES, 20 mM NaCl, 10 mM EDTA, 0,5% BSA), stained with Hoechst 33342 (10 μg/mL) at 37 °C for 30 min and washed with ice-cold PBS with BSA (0.5%). The cells were immediately analyzed using a BD FacsVerse flow cytometer (BD Biosciences, USA). The excitation wavelength for PIR was 488 nm and the emission was measured through a 586BP42 pass filter; the Hoechst 33342 was excited at 405 nm and the emission was detected through a 448BP45 filter. The data were analyzed in two independent experiments. The medians of the fluorescence intensities were calculated using FlowJo software (Tree Star, USA).

Synthesis of Monomers. *N*-(2-Hydroxypropyl)methacrylamide (HPMA) was synthesized by reacting methacryloyl chloride with (*RS*)-1-aminopropan-2-ol in dichloromethane in the presence of sodium carbonate as described.[28]

N-(tert-butoxycarbonyl)-*N*′-(6-methacrylamidohexanoyl)hydrazine (Ma-Ahx-NHNH-Boc) was prepared in a two-step process by the reaction of methacryloyl chloride with 6-aminohexanoic acid in the presence of NaOH followed by the condensation of formed 6-(methacryloylamino)hexanoic acid with *tert*-butyl carbazate in the presence of DCC.[29]

N-Methacryloylglycylphenylalanylleucylglycine (Ma-GFLG-OH) was prepared by automated solid phase peptide synthesis on 2-chlorotrityl chloride resin starting from the C-terminus using standard Fmoc procedures. 3-(*N*-Methacryloylglycylphenylalanylleucylglycine)-thiazolidine-2-thione (Ma-GFLG-TT) was prepared by reacting Ma-GFLG-OH with 4,5-dihydrothiazole-2-thiol in dimethylformamide (DMF) in the presence of DCC according to ref 30.

Synthesis of Diblock Copolymer Precursors PP2−PP4. The thermoresponsive micelle-forming polymer precursors were produced as A−B type diblock copolymers by RAFT polymerization in two synthetic steps. The hydrophilic block A was prepared by copolymerizing HPMA with Ma-Ahx-NHNH-Boc using CPB as a chain transfer agent and AIBN as an initiator. The hydrophilic block A was subsequently subjected to a chain-extension polymerization through the RAFT mechanism with DEGMA to introduce the thermoresponsive polymer block B. Three different ratios of poly[(HPMA)-*co*-(Ma-Ahx-NHNH-Boc)], as the macro-chain transfer agent, to DEGMA were used to synthesize the diblock polymers with variable lengths of the thermoresponsive blocks.

Example: A mixture of 5.8 mg of CPB (26.1 μmol) and 2.1 mg of AIBN (13.0 μmol) was dissolved in 0.368 mL of DMSO and added to a solution of 500.0 mg of HPMA (3.49 mmol) and 57.6 mg of Ma-Ahx-NHNH-Boc (0.18 mmol) in 3.312 mL of *tert*-butanol. The reaction mixture was thoroughly bubbled with Ar and polymerized in sealed glass ampules at 70 °C for 6 h. The resulting copolymer was isolated by precipitation into a 3:1 mixture of acetone and diethyl ether and purified by gel filtration using a Sephadex LH-20 cartridge in methanol. The methanolic solution was concentrated under reduced pressure and precipitated in diethyl ether yielding 268.3 mg (48.1%) of the poly[(HPMA)-*co*-(Ma-Ahx-NHNH-Boc)] polymer precursor (PP1) as a pink powder. The content of dithiobenzoate (DTB) end groups was nDTB = 60.3 μmol/g, corresponding to $M_{n,UV}$ = 16 580 g/mol (f = 0.85). Next, a solution of 50.0 mg of **PP1** (3.01 μmol DTB groups) in 64.8 μL of deionized H_2O was added to a mixture of 21.6 mg of DEGMA (0.12 mmol) and 0.1 mg of AIBN (0.60 μmol) in 130 μL of 1,4-dioxane, thoroughly bubbled with Ar and allowed to polymerize in the sealed glass ampules at 70 °C for 18 h. The diblock polymer was isolated by precipitation to diethyl ether, yielding 63.8 mg (89.1%) of pale pink amorphous solid. The precipitated polymer was dissolved in 638 μL of DMSO, 16.0 mg of ABIN (97.4 μmol) was added, and the solution was heated up to 80 °C for 2 more hours. The resulting diblock copolymer was isolated by precipitation in diethyl ether and purified by gel filtration using the Sephadex LH-20 cartridge in methanol. The methanolic solution was concentrated under vacuum and precipitated in diethyl ether yielding 52.1 mg of the poly-[(HPMA)-*co*-(Ma-Ahx-NHNH-Boc)]-*block*-p(DEGMA) polymer as a white amorphous solid. The diblock copolymer with Boc-protected hydrazide groups was suspended in 700 μL of TFA/TIPS/H_2O (92:2.5:2.5) mixture and sonicated until all solids were dissolved (∼5 min). Thereafter, the polymer was precipitated into diethyl ether and redissolved in phosphate buffer (0.15 M, pH 8.0). The pH of the solution was adjusted to 7.4 using a NaOH solution and the polymer was desalted by the Sephadex PD-10 column in H_2O. The resulting polymer precursor poly[(HPMA)-*co*-(Ma-Ahx-$NHNH_2$)]-*block*-p-(DEGMA) (**PP2**) was isolated from an aqueous solution by lyophilization yielding 48.3 mg of the white solid. The reaction conditions for all synthesized polymer precursors (**PP1−PP4**) as well as their physicochemical characteristics are summarized in Table 1.

Synthesis of Hydrophilic Copolymer Precursor PP6. The copolymer precursor poly[(HPMA)-*co*-(Ma-GFLG-TT)] (**PP6**) was prepared by RAFT polymerization of 200.0 mg of HPMA (1.40 mmol) and 87.0 mg of Ma-GFLG-TT (0.15 mmol) using 0.64 mg AIBN (3.90 μmol) as an initiator and 1.72 mg of CTP (6.16 μmol) as a chain transfer agent. The polymerization mixture was dissolved in 1.563 mL of *tert*-butanol with 10% DMSO, transferred into a glass ampule, bubbled with Ar and sealed. After 24 h at 70 °C, the product was isolated by precipitation of the reaction mixture to acetone/diethyl ether (3:1); the precipitate was then washed with diethyl ether and dried under vacuum. This product was then reacted with AIBN (10 molar excess) in DMSO (15% w/w solution of polymer) under Ar for 3 h at 70 °C in a sealed ampule to remove DTB end groups. The reaction mixture was isolated by precipitation in acetone/diethyl ether (3:1); the precipitate was washed with diethyl ether and dried under vacuum to yield 186.5 mg of copolymer precursor **PP6**. The number-average molecular weight (M_n) of the copolymer was 35 500 g/mol, and the polydispersity index ($Đ$) was 1.12. The content of TT groups (φ^{TT}) was 6.8 mol %.

Attachment of PIR and Fluorophore to the Diblock Copolymer Precursors (PC2F−PC4F). Pirarubicin was attached to the hydrazide groups distributed along the hydrophilic block A of the copolymer precursors through the hydrolytically degradable hydrazone bond. For the FACS analysis (see above), some of the hydrazide groups of the copolymers were used for the copolymer labeling with a fluorescent dye via the stable diacylhydrazine bonds.

Example: A mixture of 20.0 mg of **PP2** and 0.4 mg of DY-676 NHS-ester (0.44 μmol) was dissolved in 80 μL of DMA, and the solution was stirred for 4 h at room temperature (r.t.). Then, 2.2 mg of PIR (3.5 μmol) in 80 μL of methanol and 8 μL of acetic acid was added dropwise, and the reaction mixture was stirred for another 18 h at r.t. The resulting polymer conjugate (**PC2-F**) was separated from the reaction mixture by gel filtration using the Sephadex LH-20 column in methanol followed by inspissation of the methanolic solution on a rotary evaporator and precipitation of the conjugate in ethyl acetate, yielding 12.6 mg of the dark violet solid. The physicochemical characteristics for the polymer−PIR conjugates are summarized in Table 2.

DOI: 10.1021/acs.biomac.5b00764
Biomacromolecules XXXX, XXX, XXX−XXX

Scheme 1. Synthesis of Amphiphilic Diblock Copolymer Precursors PP1–PP4 Using the RAFT Polymerization Technique

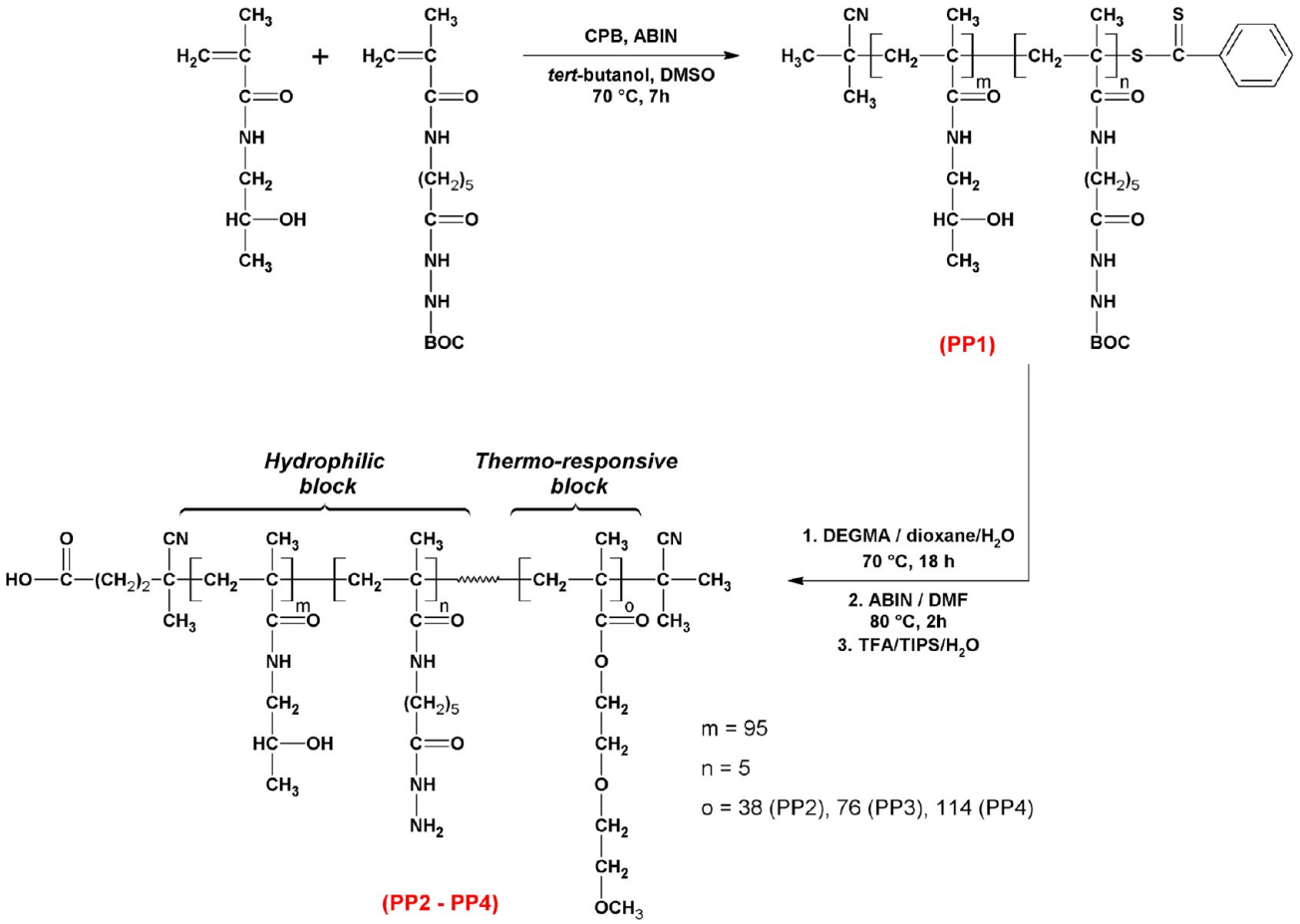

Attachment of PIR to the Hydrophilic Copolymer Precursor (PC6). A mixture of 92.0 mg of **PP6** (36.5 μmol TT) and 7.9 mg of PIR (12.6 μmol) was dissolved in 1.75 mL of DMA and stirred at r.t. The yield of the reaction was monitored by HPLC. After 3 h, when the reaction was completed, 4.3 μL of (*RS*)-1-aminopropan-2-ol (54.8 μmol) was added to the reaction mixture to quench the unreacted TT. After another 30 min, the polymer conjugate was isolated by precipitation of the reaction mixture in ethyl acetate and the precipitate was centrifuged. The precipitate was washed with diethyl ether and dried under vacuum yielding 84.0 mg of **PC6**. M_n = 41 000 g/mol, $Đ$ = 1.17, and ω^{PIR} = 9.0 wt %. The chemical structure of **PC6** conjugate is shown in Supporting Information Figure S1B.

RESULTS AND DISCUSSION

Polymer–PIR Conjugates Synthesis. The synthesis of the polymer–PIR conjugates was carried out in two synthetic steps, including the synthesis of the amphiphilic diblock copolymer precursors, followed by the attachment of either the cancerostatic drug pirarubicin or the fluorescent dye. The precursors (**PP1–PP4**) were synthesized by the RAFT polymerization technique, enabling the synthesis of highly defined uniform materials with predetermined molecular weights and high yield of DTB end-group content. The hydrophilic block (PP1) was prepared by copolymerizing HPMA with Ma-Ahx-NHNH-Boc using the DTB-derived chain transfer agent (see Scheme 1). The copolymer with M_n = 14 100 g/mol was distinguished by narrow molecular weight distribution (M_w/M_n = 1.11) and sufficient functionality (f = 0.85) of the DTB end groups. The functionality of the polymer (f, the amount of the functional end groups per one polymer chain) was defined as the ratio between M_n obtained from the SEC measurement and $M_{n,UV}$ calculated from the end group analysis. The content of comonomer units bearing the hydrazide groups, determined by TNBSA assay (after removal of Boc protective groups, see Experimental Section) and confirmed by ^{1}H NMR spectroscopy (data not shown) was 4.8 mol %, which is equal (within experimental error) to the quantity of Ma-Ahx-NHNH-Boc (5.0 mol %) in the polymerization feed. The precursor **PP1** was further used as the macro-chain transfer agent for the subsequent chain extension with the thermoresponsive poly(DEGMA) blocks. Three different ratios of DEGMA to DTB-end groups of **PP1** were used (see Table 1) to synthesize the amphiphilic diblock copolymers with variable lengths of the thermoresponsive block ranging from approximately 7000 to 24 600 g/mol. The incorporation of poly(DEGMA) blocks to the HPMA-based copolymer precursor resulted in a moderate broadening of the distribution of molecular weights ($M_w/M_n \approx 1.5$). This can be ascribed to a low but not insignificant quantity of **PP1** dead chains (not terminated with DTB groups) that could not react further with DEGMA through the RAFT mechanism. Consequently, the resulting precursors were the mixture of two polymer populations with different molecular weights: the largely prevailing diblock copolymer, and a small amount of initial hydrophilic precursor (Figure 1).

To prevent the unwanted reactions of DTB end groups of the polymers with the hydrazide side chain groups during the removal of Boc protective groups or with PIR during the following conjugation, the DTB groups were removed by a

DOI: 10.1021/acs.biomac.5b00764
Biomacromolecules XXXX, XXX, XXX–XXX

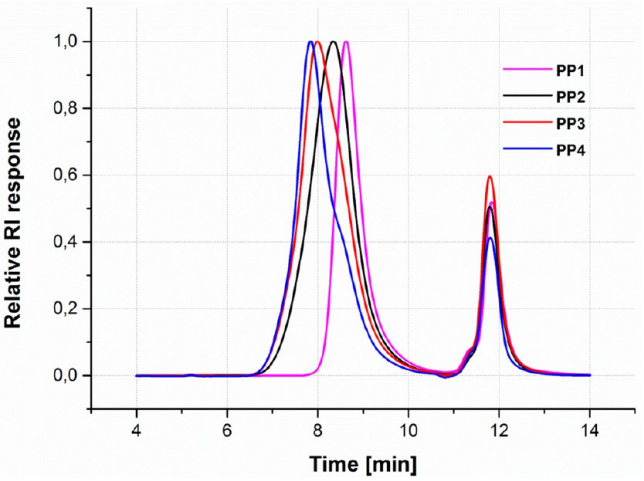

Figure 1. SEC profiles of the copolymer precursors **PP1**−**PP4** plotted as a function of time of the normalized RI responses.

reaction with a high molar excess of AIBN through the homolytic mechanism. The replacement of DTB groups by the isobutyronitrile groups was documented by the disappearance of the UV absorption peak at 302 nm. Finally, Boc groups protecting the hydrazides were quantitatively removed using the TFA/TIPS/H_2O mixture, commonly used in peptide chemistry, yielding the polymer precursors **PP2**−**PP4**. Neither the DTB group substitution nor the removal of Boc groups caused significant changes in the molecular weights and molecular weight distributions of the polymer precursors. The molecular weight parameters for **PP2**−**PP4** are summarized in Table 1, and SEC profiles are depicted in Figure 1.

The conjugation of PIR to the copolymer precursors was achieved by the hydrazone bonds formed between the keto group of PIR and the hydrazide groups in the side chains of polymers (the reaction scheme is shown in Scheme 2; an example of SEC chromatogram for the conjugate **PC2** recorded by LS, RI, and UV detectors is depicted in Figure S2B). Based on our previous experiences with the structurally similar cancerostatic drug doxorubicin (DOX), the reaction was performed in methanol in the presence of acetic acid.[31] The

Scheme 2. Conjugation of PIR and DY-676 Fluorescent Dye with Diblock Copolymer Precursors PP2−PP4 through the Hydrazone and Diacylhydrazine Bond, Respectively[a]

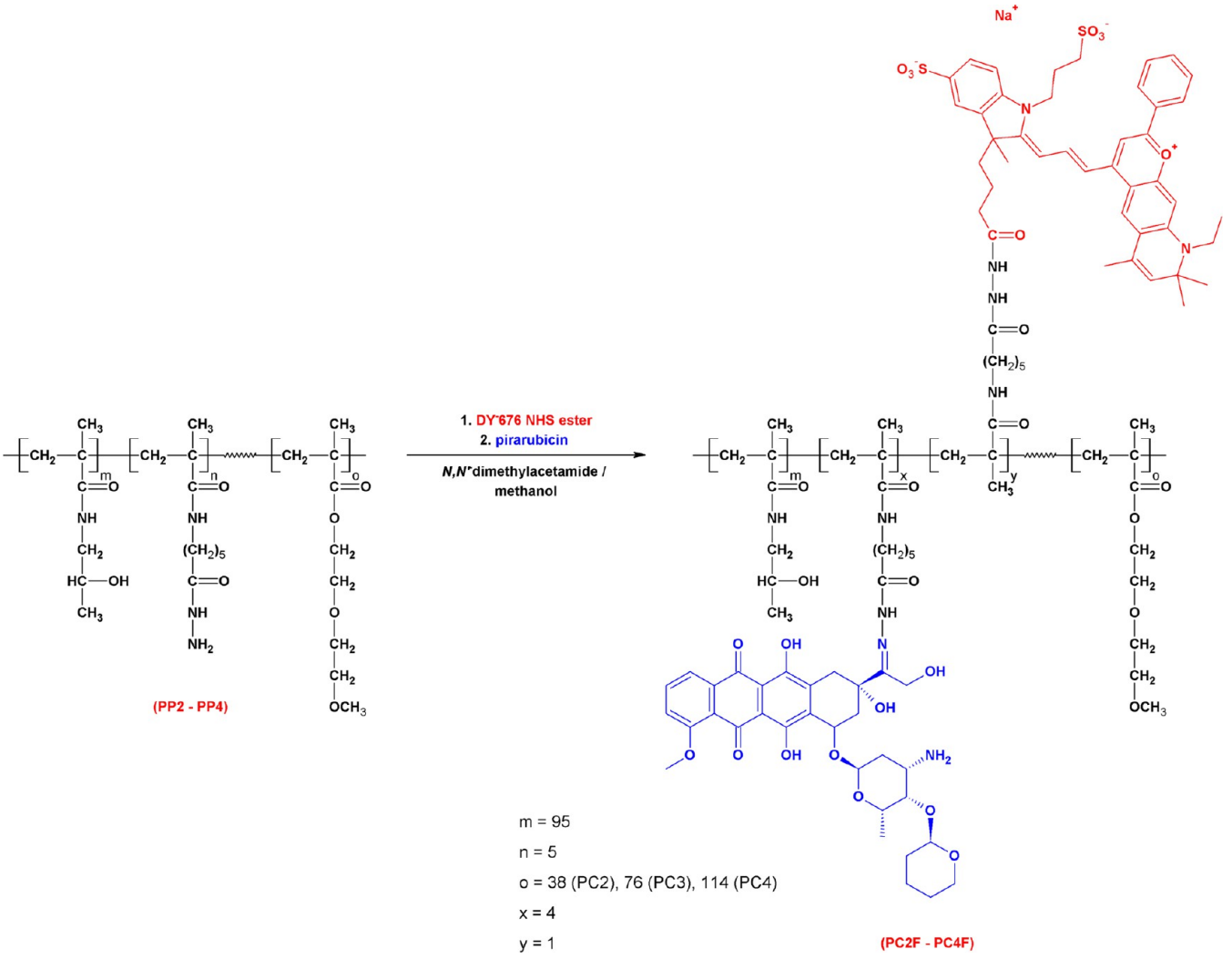

[a]Conjugates **PC2**−**PC4** were prepared analogously in the absence of DY-676.

DOI: 10.1021/acs.biomac.5b00764
Biomacromolecules XXXX, XXX, XXX−XXX

yields of the conjugation reaction ranged between 70 and 80%. The method of PIR attachment was selected with respect to the pH-controlled stability of the hydrazone bond—relatively stable at neutral pH but susceptible to much faster hydrolysis in mildly acidic conditions. This approach is very beneficial for a systemic administration because the majority of the drug remains attached to the polymer carrier during its transport in the bloodstream (pH 7.4) but is released in the target tumor cells (pH 5.5). To verify this claim, we measured the release of PIR from conjugates **PC2—PC4** under physiological environment-modeling conditions (see Experimental Section) at both relevant pH values. As shown in Figure 2A, the rate of the

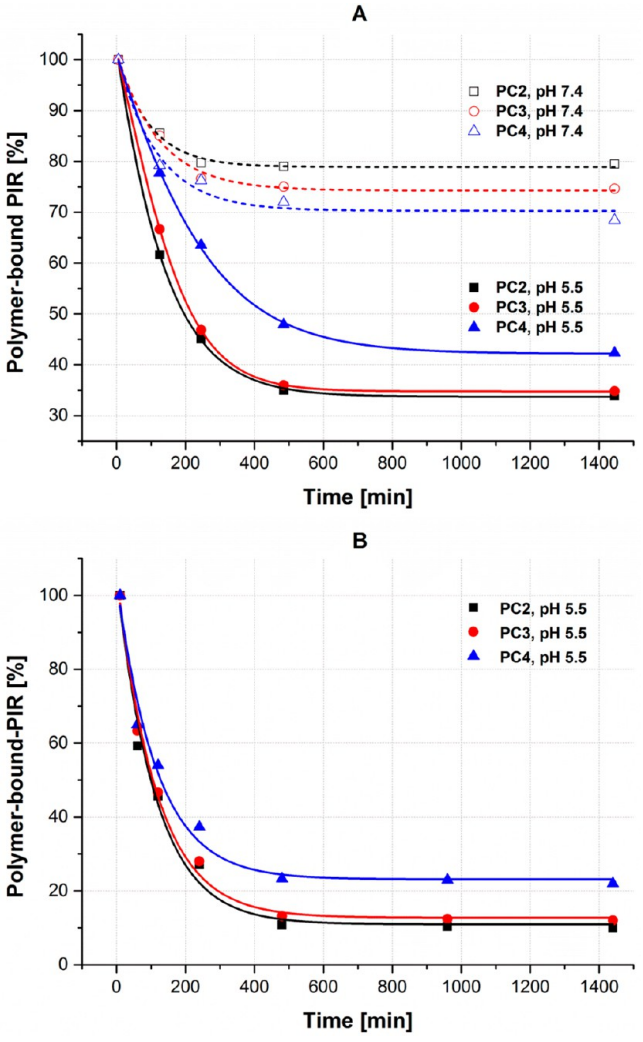

Figure 2. Release of PIR from the polymer—PIR conjugates **PC2—PC4** incubated in phosphate buffers at pH 7.4 (dashed lines) and pH 5.5 (solid lines) at 37 °C. Quantification of the polymer-bound PIR was performed using the UV/vis spectrophotometry by measuring the absorbance of the polymer—PIR conjugates separated from free PIR by GPC carried out either in (A) PBS or in (B) methanol/sodium acetate buffer (80:20) mixture.

hydrazone bond hydrolysis proceeded much faster in solutions with a lower pH, which documents the suitability of the conjugates for safe drug delivery purposes. Although the ability of the conjugates to release PIR under the conditions modeling the intratumoral environment is evident, it appears that the conjugates in aqueous solution still contain approximately 35—40% of bound PIR even after 24 h of acidic hydrolysis at pH 5.5. This can be explained by the hydrophobic character of the poly(DEGMA) chains retaining the already released hydrophobic drug packed inside the polymer coil by hydrophobic interactions upon disruption of the hydrazone bond. The hydrophobic retention of PIR by the polymer coil increased with increasing poly(DEGMA) block length. The release of PIR was also evaluated by GPC analysis with the methanol/sodium acetate buffer (80:20) mixture as a mobile phase (see Experimental Section). In the methanolic solution, the hydrophobic interaction between the polymer and the released drug was disrupted, which resulted in an almost complete release of PIR from the carrier by hydrolysis (see Figure 2B).

For the LSCM measurement of the interaction of the conjugates with the cells, the polymer precursors **PP2—PP4** were modified (in a one-pot reaction together with PIR) with DY-676 NHS ester fluorescent dye (**PC2F—PC4F**) that emits light in a different region of the light spectrum than PIR (see Experimental Section). Because the fluorescent dye was attached to the polymer backbone of the conjugates through the stable diacylhydrazine bonds (see Scheme 2), the LSCM images enabled a simultaneous observation of the intracellular fate of the polymer and PIR (both bound and released) over time. However, we would like to note that the apparent molecular weights of the fluorescently labeled polymer—PIR conjugates, measured by GPC equipped with a LS detector, were approximately 1.5 times higher than those of the corresponding polymer precursors. Because no broadening of the molecular weight distributions was observed, we hypothesize that this difference was due to the contribution of PIR fluorescence to the intensity of the light scattering. Therefore, it was necessary to calculate the molecular weights by a "relative" molecular weight determination method using a series of well-characterized poly(HPMA) polymer standards. The molecular weights of such characterized conjugates were only approximately 3—5% higher than those of the corresponding precursors, which is in good agreement with the theoretical expectation. Complete physicochemical characteristics of the polymer—PIR conjugates, including the corrected molecular weights (MWs) are summarized in Table 2.

Solution Behavior of Thermoresponsive Polymer—PIR Conjugates. The temperature-dependent changes in solution behavior of the polymer—PIR conjugates and their corresponding precursors were studied by DLS. We focused on the influence of the composition and structural parameters of the polymers on their hydrodynamic properties in the solutions mimicking physiological conditions as our understanding of such properties may play an important role in the design of drug delivery systems for efficient in vivo treatment. First, we clearly demonstrated that the hydrophobic poly(DEGMA) block length (MW) is the decisive structural factor. Specifically, an increase in molecular weight of the poly(DEGMA) block (at a constant MW of the hydrophilic block) caused not only a decrease in transition temperatures (T_{tr}) of the copolymers but also resulted in the formation of larger-sized polymer coils (below T_{tr}) and larger-sized polymer micelles (above T_{tr}) (see Figure 3). For example, the **PP2** precursor with MW of the hydrophilic block almost 2 times higher than the hydrophobic block showed a T_{tr} 18 °C higher than poly(DEGMA) homopolymer ($T_{tr} \approx 26$ °C), while in the case of **PP4**, where the MW of the hydrophobic block is 1.7 times higher than the MW of the hydrophilic block, the T_{tr} of the copolymer is only slightly higher in comparison to poly(DEGMA) itself.

DOI: 10.1021/acs.biomac.5b00764
Biomacromolecules XXXX, XXX, XXX—XXX

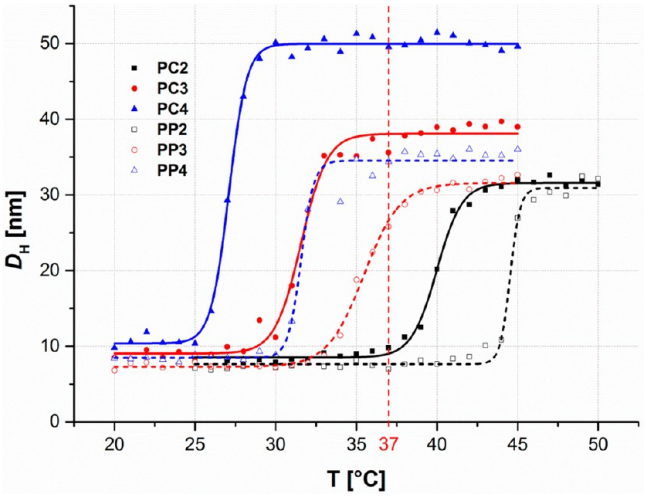

Figure 3. Temperature dependence of the hydrodynamic diameters (D_H) of polymer–PIR conjugates **PC2–PC4** (solid lines) and their corresponding precursors **PP2–PP4** (dashed lines) measured by DLS.

Based on these observations (and also our understanding of the dependence of T_{tr} on MW of other thermoresponsive polymers), it is reasonable to predict that further poly(DEGMA) chain lengthening would not result in significant T_{tr} decrease. Additionally, an increase in the polymer micelle sizes of the **PC2–PC4** conjugates with increasing MW of poly(DEGMA) chains was predictable because longer polymer chains self-assembled into larger-sized nanoparticles. The length of the hydrophobic block has also an impact on the micelle stabilities expressed by the critical micellar concentration (CMC) values. It was shown that the CMC values decreased (stabilities of the conjugates increased) with increasing MW of the poly(DEGMA) blocks from 0.071 mg/mL for **PC2** up to 0.022 mg/mL for **PC4**. Considering the usual concentrations (~10 mg PIR/kg of mouse body weight, *i.v.* injection) of the previously described polymer–PIR conjugates in mice experiments,[32] the CMC values acquired for **PC2–PC4** guarantee, with a sufficient reserve, that the thermoresponsive conjugates will exist in their micellar form even after their injection to the mice. This interesting finding brought a comparison of T_{tr} of the polymer precursors and the polymer–PIR conjugates. As shown in Figure 3, the incorporation of the hydrophobic drug to the polymers caused a marked decrease in T_{tr} (by ~5 °C) regardless of the poly(DEGMA) block length. Because PIR is attached to the polymers through hydrolytically degradable bonds, it is reasonable to expect that T_{tr} of the conjugates will increase upon PIR release inside the cells (an example of increase of T_{tr} of the conjugate **PC2** after 24 h of hydrolysis carried out under model conditions (PBS, pH 5.5, 37 °C) is shown in Figure S3). This increase in T_{tr} can be employed in the design of biodegradable micelle-based drug delivery systems. Such drug-bearing conjugates can reach the target tumor cells in their micellar form (T_{tr} < 37 °C) through the EPR effect, but the drug-free copolymer (T_{tr} > 37 °C) can be reliably eliminated from the body as an unimer (single copolymer molecules) formed upon PIR release, through renal filtration. From this point of view, the conjugate **PC3** exhibited the most favorable properties. It formed a polymer micelle spontaneously under physiological conditions, but began to change its morphology to random coil during PIR cleavage from the polymer. As shown at Figure 4, polymer conjugate **PP3** (the precursor of **PC3**) at 37 °C is predominantly in the micellar form; however,

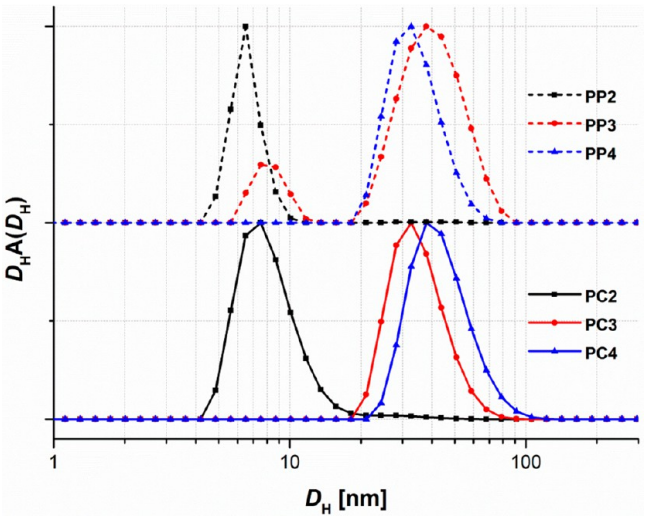

Figure 4. Normalized D_H-distribution function, $A(D_H)$, of polymer–PIR conjugates **PC2–PC4** (solid lines) and their corresponding precursors **PP2–PP4** (dashed lines) measured by DLS.

a significant portion of the polymer is present already in the form of unimers. To the contrary, the conjugate **PC2** adopted the random coil formation both before and after PIR release, and the conjugate **PC4** existed only as a fully solvated unimer regardless of attached or released PIR (see Figures 3 and 4).

Cytotoxicities of the Polymer–PIR Conjugates. The cytotoxicities of PIR and the polymer–PIR conjugates were reported as IC_{50} values, which is the concentration of material at which 50% of the cell culture is no longer viable. In this experiment, we used the human colorectal adenocarcinoma (DLD-1) and the mouse lymphoma (EL-4) cell lines, both relevant models to this study. According to the results in Table 3, the IC_{50} values of the thermoresponsive polymer–PIR conjugates **PC2–PC4** are all very similar (approximately 3 μg/mL against DLD-1 cell line and 0.01 μg/mL against EL-4 cell line). However, these values are approximately 20 times higher (in the case of DLD-1 cells) than those for free PIR. This finding demonstrates that the attachment of the drug to the polymer carriers significantly reduces its direct cytotoxicity and, at the same time, that the poly(DEGMA) block length nowise affects the toxicity of the conjugates. Lower conjugate toxicity is favorable because it enables the administration of the drug at a higher concentration, thus increasing the potential therapeutic effect. The comparison of the thermoresponsive polymer–PIR conjugates **PC2–PC4** with the linear hydrophilic polymer–PIR conjugates containing the drug attached to the polymer backbone either through the hydrolytically degradable hydrazone bond (**PC5**) or through the enzymatically degradable tetrapeptide spacer GFLG (**PC6**) led to interesting results. While the cytotoxicity of the conjugate **PC5** was approximately 2 times (for the DLD-1 cells) or 100 times (for the EL-4 cells) higher than that for **PC2–PC4** (not statistically significant differences), the conjugate **PC6** was approximately 5 times less toxic (for DLD-1 cells) than the thermoresponsive ones (statistically significant differences). The higher toxicity of the **PC5** conjugate can be ascribed to the more hydrophilic character of its polymer backbone enabling faster release of PIR from the carrier without its subsequent retention due to

DOI: 10.1021/acs.biomac.5b00764
Biomacromolecules XXXX, XXX, XXX–XXX

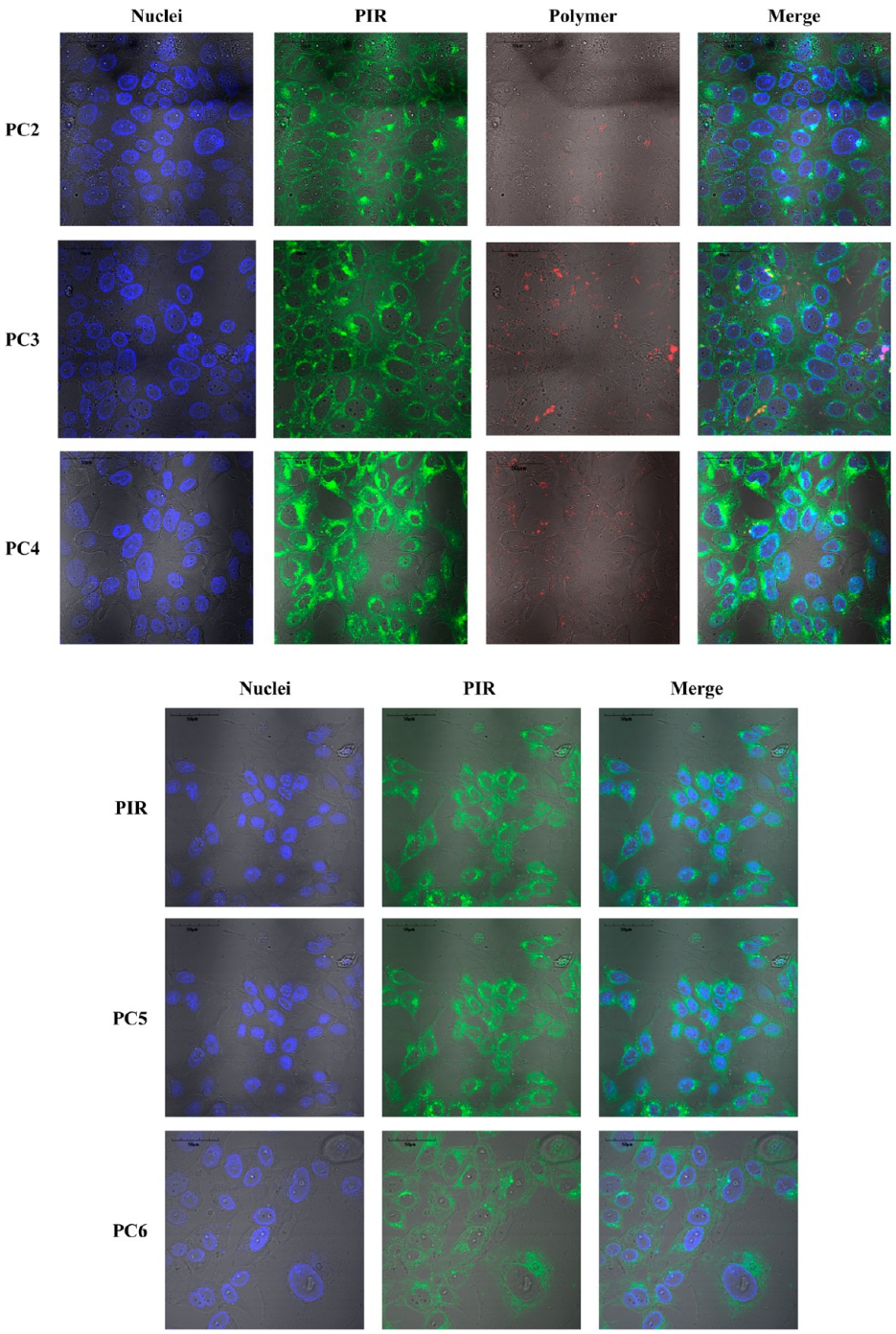

Figure 5. LSCM images of polymer−PIR conjugates and free PIR in DLD-1 cell lines after 24 h of incubation. Hoechst 333258 dye was used for the visualization of cell nuclei (blue color) and Dyomics-676 dye was used for the visualization of the polymers (red color). Green color represents PIR.

hydrophobic interaction with the hydrophobic block of the copolymer (see ref 33). To the contrary, conjugate **PC6**, although having PIR bound via the enzymatically degradable GFLG linker, released only a modest amount of the drug within the monitored time interval. This is in agreement with a published observation.[34,35] The polymer precursors **PP2**−**PP4** showed no toxicity. The pronounced differences of approximately 2 orders of magnitude in the IC_{50} values measured in DLD-1 and EL-4 cells are caused by the different sensitivities of the two cell lines to PIR.

Internalization of the Polymer−PIR Conjugates into Cells. The intracellular fate of the polymer−PIR conjugates and free PIR was observed in DLD-1 cells by LSCM at different time points (see Experimental Section). The fluorescent signal of the DY-676-labeled polymer conjugates increased over time for all studied samples. As shown in Figure 5, there are obvious differences in the intracellular localization and the mechanism of action between free PIR, the thermoresponsive polymer−PIR conjugates and the control hydrophilic polymer−PIR conjugates. While in the case of free PIR and the control polymer−PIR conjugate having PIR attached through the hydrolytically degradable bond (**PC5**) a substantial amount of the drug was detected in the cytoplasm and inside the cell nuclei, in the case of the thermoresponsive polymer−PIR

DOI: 10.1021/acs.biomac.5b00764
Biomacromolecules XXXX, XXX, XXX−XXX

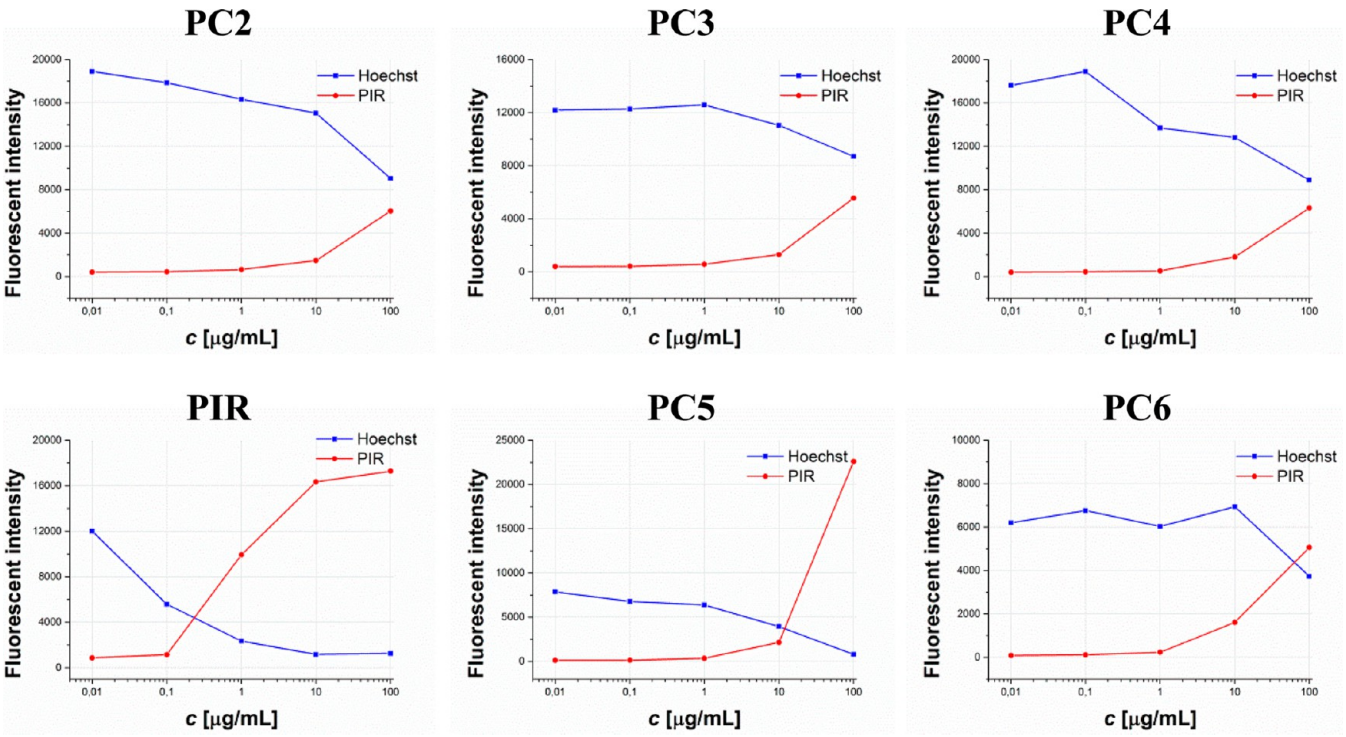

Figure 6. Incorporation of PIR released from the polymer−PIR conjugates into the DLD-1 cell nuclei evaluated from the decrease of the fluorescence intensity of Hoechst 333258 dye (blue line) or from the increase of the fluorescence intensity of PIR (red line), respectively, as a result of the intercalation competition between PIR and Hoechst 333258 dye.

conjugates (**PC2−PC4**) and the control hydrophilic polymer−PIR conjugate having PIR attached through the enzymatically degradable GFLG spacer (**PC6**), PIR was predominantly detected in the cytoplasm and on the surface of the nuclear membrane. The fact that only a very small amount of PIR was found in the cell nuclei can be probably attributed to the hydrophobic retention of the released PIR in the hydrophobic poly(DEGMA) domains of copolymers **PC2−PC4** and the relatively slow enzymatic cleavage of the GFLG tetrapeptide spacer in copolymer PC6 by lysosomal proteases.[34,35] Surprisingly, although the structure and chemical composition of the two types of conjugates (**PC2−PC4** and **PC6**) is different, their intracellular fate, according to the LSCM study, seems to be quite similar. These polymer/PIR conjugates probably interact hydrophobically with the lipid bilayer of the cell nucleus, thereby decreasing the membrane permeability and preventing further progression of the cells. LSCM showed that the cells incubated with the **PC2−PC4** and **PC6** conjugates significantly changed their morphology and size of the intracellular compartments, namely, the nuclei, in comparison with the nontreated cells (not shown) and the cells treated with PIR or **PC5** conjugate. This behavior of the cells resembles the phenomenon called oncosis, a nonapoptotic mode of cell death, characterized by mitochondrial swelling, cytoplasm vacuolization, and swelling of the nucleus and cytoplasm.[37] Moreover, the cells treated with **PC2 − PC4** and **PC6** conjugates showed reduced amount of the mutual intracellular connections documenting an apparent damage of the cells. Because the polymer precursors **PP2−PP4** without PIR were nontoxic and did not affect the morphology of the cancer cells (LSCM images not shown), it is obvious that the polymer carriers alone were not responsible for the observed cytotoxic effect of the conjugates. In this experimental setting, no pronounced difference in the behavior of cells treated with individual thermoresponsive polymer−PIR conjugates **PC2−PC4** and polymer **PC6** on the cancer cells was observed. It appears that the poly(DEGMA) block, regardless of its length, is the principal structural factor of the polymer−PIR conjugates influencing their biological behavior. As already mentioned, despite the significant structural differences between the thermoresponsive polymer−PIR conjugates **PC2−PC4** and hydrophilic polymer−PIR conjugate **PC6**, the LSCM images documenting the intracellular fate of the conjugates are strikingly similar. We can hypothesize that both types of conjugates exhibit an amphiphilic character (due to the presence of thermoresponsive poly(DEGMA) block in conjugates **PC2−PC4** and a hydrophobic GFLG spacer between PIR and polymer backbone in conjugate **PC6**) that might be responsible for the nonspecific interaction of the polymer conjugates with various membrane structures inside the cells. The detailed analysis of the intracellular behavior of the conjugates and the mechanism of their action in the cancer cells will be the subject of our upcoming publication.

Incorporation of PIR into the Cell Nuclei. To verify the results from LSCM images, the Hoechst incorporation assay using FACS analysis was performed. The cells (DLD-1) were incubated with a concentration array of the polymer−PIR conjugates or free PIR for 24 h followed by the addition of Hoechst 33342, an intercalating fluorescent dye used for DNA staining. The assay is based on the characteristics of PIR to intercalate between the base pairs of DNA strands and thus block the subsequent interaction of DNA with Hoechst. In other words, the Hoechst dye can insert only in sections of DNA strands that are not occupied by PIR. The results of intercalating competitions between the DNA/PIR complexes and the Hoechst 333258 dye for the individual polymer−PIR f6

DOI: 10.1021/acs.biomac.5b00764
Biomacromolecules XXXX, XXX, XXX−XXX

conjugates as well as for free PIR are shown in Figure 6. The highest intercalation ability showed free PIR whose concentration in the cell nuclei gradually increased (the concentration of Hoechst in the cell nuclei gradually decreased) from 1 μg/mL to 100 μg/mL, at which point almost all intercalating sites of DNA were occupied by PIR (no Hoechst was detected). A slightly lower intercalation efficiency was found in the case of **PC5** conjugate, where a sharp increase in PIR fluorescence intensity was observed starting from 10 μg/mL of PIR. However, as in the previous case, DNA was fully saturated with PIR at a concentration of 100 μg/mL. This demonstrates the successful hydrolysis of the hydrazone bond, release of PIR from the conjugate, and its subsequent penetration in the nucleus. Markedly different results were obtained when the cells were incubated with the **PC6** conjugate. Although PIR started incorporating slightly in the nuclei at a concentration 1 μg/mL, the efficiency of its intercalation was relatively low, which enabled the Hoechst dye to interact with DNA too. Only in the case of the highest concentration of the conjugate (100 μg/mL of PIR) did the amount of incorporated Hoechst decrease. This can be ascribed to a very low rate of PIR release from the conjugate due to the relatively slow gradual enzymatic cleavage of the GFLG spacer between the drug and the polymer backbone[34,35] and possibly also the hydrophobic retention of the released drug within the polymer coil containing amphiphilic GFLG peptides. Similar results were also observed in cells incubated with the thermoresponsive **PC2**−**PC4** conjugates. In all cases, the Hoechst dye was incorporated in DNA in the entire range of concentration of the conjugates (0.01−100 μg/mL of PIR), indicating the low level of PIR intercalated in the cell nuclei even at the highest conjugate concentration. These results are in good agreement with the LSCM pictures, in which almost no PIR signal from the **PC2**−**PC4** conjugates was detected inside the nuclei. This confirms our hypothesis that PIR remains hydrophobically entrapped inside the coil of the thermoresponsive polymers even after the hydrazone bond hydrolysis inside the cells. Furthermore, it seems that this interaction is independent of the poly(DEGMA) block length, or more precisely, of the conjugate morphology.

CONCLUSION

Conjugates of nanosized polymer carriers with chemotherapeutics are considered to be a very promising drug delivery system intended for the treatment of neoplastic diseases. The major benefit is in their high ability for passive accumulation in solid tumors due to the EPR effect, while causing minimal damage to healthy tissues. However, the clinical application of the majority of the nanoparticle-based carriers encounters obstacles related to their relatively laborious preparation, high tendency to aggregate, limited drug loading, and complicated long-term storage. Therefore, in this work, we focused on the development of novel thermoresponsive polymer carriers characterized by relatively easy and reproducible preparation, precisely defined chain structure with multiple binding sites for covalent attachment of drugs, an adjustable unimer−micelle transition temperature, and long-term stability. The diblock polymer carriers, synthesized by RAFT polymerization, were comprised of a multivalent HPMA-based hydrophilic block and a thermoresponsive DEGMA-based block of various lengths. The cancerostatic drug pirarubicin (PIR) was conjugated to the hydrophilic blocks of the copolymers via a hydrolytically cleavable hydrazone bond. The polymer−PIR conjugates showed spontaneous pH-driven hydrolysis of the hydrazone bonds; PIR release proceeded much faster at pH 5.5, corresponding to the intracellular environment than at pH 7.4, corresponding to the blood circulation, thus meeting the requirements for safe delivery of the drug to cancer cells. The conjugates underwent reversible temperature-induced conformation changes from random coils to stable nanosized micelles; the micelle size and stability as well as the transition temperature of the conjugates were driven by the thermoresponsive block length and PIR content in the range of 26 to 39 °C. All studied conjugates, regardless of thermoresponsive block length, showed significantly lower cytotoxicity than free PIR (both in DLD-1 and EL-4 cells) and demonstrated the ability to effectively penetrate the cell membrane of model cancer cell lines (DLD-1). Although a considerable amount of PIR remained hydrophobically attached to the polymer carrier even after the hydrazone bond disruption inside the cells, the resulting polymer/PIR associates surrounded the cell nuclei membranes and blocked the transport through the membrane. This led to changes in cell morphology and disrupted mutual intracellular connections, indicating approaching cell death. Based on these encouraging results, we believe that the studied conjugates have a great potential to become efficacious in vivo pharmaceuticals.

ASSOCIATED CONTENT

Supporting Information

The Supporting Information shows chemical structures of the polymer conjugates **PC5** and **PC6**, examples of the detailed SEC profiles for the polymers **PP2** and **PC2**, and comparison ot the temperature dependences of the polymer conjugate **PC2** before and after hydrolysis. The Supporting Information is available free of charge on the ACS Publications website at DOI: 10.1021/acs.biomac.5b00764.

AUTHOR INFORMATION

Corresponding Author

*E-mail: laga@imc.cas.cz.

Author Contributions

The manuscript was written through contributions of all authors. All authors have given approval to the final version of the manuscript.

Notes

The authors declare no competing financial interest.

ACKNOWLEDGMENTS

This work was financially supported by a grant of Ministry of Education, Youth and Sports of the Czech Republic (Grant No. EE2.3.30.0029) and by BIOCEV (CZ.1.05/1.1.00/02.0109) - Biotechnology and Biomedicine Centre of the Academy of Sciences and Charles University from the European Regional Development Fund.

REFERENCES

(1) Hill, A. V.; Reyes-Sandoval, A.; O'Hara, G.; Ewer, K.; Lawrie, A.; Goodman, A.; Nicosia, A.; Folgori, A.; Colloca, S.; Cortese, R.; Gilbert, S. C.; Draper, S. J. Prime-boost vectored malaria vaccines: progress and prospects. *Hum. Vaccines* **2010**, *6* (1), 78−83.

(2) Satchi-Fainaro, R.; Duncan, R.; Barnes, C. M. Polymer therapeutics for cancer: Current status and future challenges. In *Polymer Therapeutics II*; Satchi-Fainaro, R., Duncan, R., Eds.; Advances in Polymer Science Series; Springer-Verlag: Berlin Heidelberg, 2006; Vol. *193*, pp 1−65.

DOI: 10.1021/acs.biomac.5b00764
Biomacromolecules XXXX, XXX, XXX−XXX

(3) Matsumura, Y.; Maeda, H. A New Concept for Macromolecular Therapeutics in Cancer-Chemotherapy - Mechanism of Tumoritropic Accumulation of Proteins and the Antitumor Agent Smancs. *Cancer Res.* **1986**, *46* (12), 6387−6392.
(4) Maeda, H. Macromolecular therapeutics in cancer treatment: The EPR effect and beyond. *J. Controlled Release* **2012**, *164* (2), 138−144.
(5) Maeda, H.; Nakamura, H.; Fang, J. The EPR effect for macromolecular drug delivery to solid tumors: Improvement of tumor uptake, lowering of systemic toxicity, and distinct tumor imaging in vivo. *Adv. Drug Delivery Rev.* **2013**, *65* (1), 71−79.
(6) Etrych, T.; Jelinkova, M.; Rihova, B.; Ulbrich, K. New HPMA copolymers containing doxorubicin bound via pH-sensitive linkage: synthesis and preliminary in vitro and in vivo biological properties. *J. Controlled Release* **2001**, *73* (1), 89−102.
(7) Rejmanova, P.; Kopecek, J.; Pohl, J.; Baudys, M.; Kostka, V. Polymers Containing Enzymatically Degradable Bonds 0.8. Degradation of Oligopeptide Sequences in N-(2-Hydroxypropyl)-Methacrylamide Co-Polymers by Bovine Spleen Cathepsin-B. *Makromol. Chem.* **1983**, *184* (10), 2009−2020.
(8) Shen, W. C.; Ryser, H. J. P. Cis-Aconityl Spacer between Daunomycin and Macromolecular Carriers - a Model of Ph-Sensitive Linkage Releasing Drug from a Lysosomotropic Conjugate. *Biochem. Biophys. Res. Commun.* **1981**, *102* (3), 1048−1054.
(9) Etrych, T.; Subr, V.; Strohalm, J.; Sirova, M.; Rihova, B.; Ulbrich, K. HPMA copolymer-doxorubicin conjugates: The effects of molecular weight and architecture on biodistribution and in vivo activity. *J. Controlled Release* **2012**, *164* (3), 346−54.
(10) Etrych, T.; Kovar, L.; Strohalm, J.; Chytil, P.; Rihova, B.; Ulbrich, K. Biodegradable star HPMA polymer-drug conjugates: Biodegradability, distribution and anti-tumor efficacy. *J. Controlled Release* **2011**, *154* (3), 241−248.
(11) Filippov, S. K.; Chytil, P.; Konarev, P. V.; Dyakonova, M.; Papadakis, C. M.; Zhigunov, A.; Plestil, J.; Stepanek, P.; Etrych, T.; Ulbrich, K.; Svergun, D. I. Macromolecular HPMA-Based Nanoparticles with Cholesterol for Solid-Tumor Targeting: Detailed Study of the Inner Structure of a Highly Efficient Drug Delivery System. *Biomacromolecules* **2012**, *13* (8), 2594−2604.
(12) Liu, R.; Li, D.; He, B.; Xu, X. H.; Sheng, M. M.; Lai, Y. S.; Wang, G.; Gu, Z. W. Anti-tumor drug delivery of pH-sensitive poly(ethylene glycol)-poly(L-histidine-)-poly(L-lactide) nanoparticles. *J. Controlled Release* **2011**, *152* (1), 49−56.
(13) Thambi, T.; Yoon, H. Y.; Kim, K.; Kwon, I. C.; Yoo, C. K.; Park, J. H. Bioreducible Block Copolymers Based on Poly(Ethylene Glycol) and Poly(gamma-Benzyl L-Glutamate) for Intracellular Delivery of Camptothecin. *Bioconjugate Chem.* **2011**, *22* (10), 1924−1931.
(14) Batrakova, E. V.; Kabanov, A. V. Pluronic block copolymers: Evolution of drug delivery concept from inert nanocarriers to biological response modifiers. *J. Controlled Release* **2008**, *130* (2), 98−106.
(15) Meyer, D. E.; Shin, B. C.; Kong, G. A.; Dewhirst, M. W.; Chilkoti, A. Drug targeting using thermally responsive polymers and local hyperthermia. *J. Controlled Release* **2001**, *74* (1−3), 213−224.
(16) Hruby, M.; Konak, C.; Kucka, J.; Vetrik, M.; Filippov, S. K.; Vetvicka, D.; Mackova, H.; Karlsson, G.; Edwards, K.; Rihova, B.; Ulbrich, K. Thermoresponsive, Hydrolytically Degradable Polymer Micelles Intended for Radionuclide Delivery. *Macromol. Biosci.* **2009**, *9* (10), 1016−1027.
(17) Hoogenboom, R.; Thijs, H. M. L.; Jochems, M. J. H. C.; van Lankvelt, B. M.; Fijten, M. W. M.; Schubert, U. S. Tuning the LCST of poly(2-oxazoline)s by varying composition and molecular weight: alternatives to poly(N-isopropylacrylamide)? *Chem. Commun.* **2008**, *44*, 5758−5760.
(18) Bogomolova, A.; Filippov, S. K.; Starovoytova, L.; Angelov, B.; Konarev, P.; Sedlacek, O.; Hruby, M.; Stepanek, P. Study of Complex Thermosensitive Amphiphilic Polyoxazolines and Their Interaction with Ionic Surfactants. Are Hydrophobic, Thermosensitive, and Hydrophilic Moieties Equally Important? *J. Phys. Chem. B* **2014**, *118* (18), 4940−4950.
(19) Fernandez-Trillo, F.; Dureault, A.; Bayley, J. P. M.; van Hest, J. C. M.; Thies, J. C.; Michon, T.; Weberskirch, R.; Cameron, N. R. Elastin-based side-chain polymers: Improved synthesis via RAFT and stimulus responsive behavior. *Macromolecules* **2007**, *40* (17), 6094−6099.
(20) Lutz, J. F.; Akdemir, O.; Hoth, A. Point by point comparison of two thermosensitive polymers exhibiting a similar LCST: Is the age of poly(NIPAM) over? *J. Am. Chem. Soc.* **2006**, *128* (40), 13046−13047.
(21) Conrad, R. M.; Grubbs, R. H. Tunable, Temperature-Responsive Polynorbornenes with Side Chains Based on an Elastin Peptide Sequence. *Angew. Chem., Int. Ed.* **2009**, *48* (44), 8328−8330.
(22) Becer, C. R.; Hahn, S.; Fijten, M. W. M.; Thijs, H. M. L.; Hoogenboom, R.; Schubert, U. S. Libraries of Methacrylic Acid and Oligo(ethylene glycol) Methacrylate Copolymers with LCST Behavior. *J. Polym. Sci., Part A: Polym. Chem.* **2008**, *46* (21), 7138−7147.
(23) Bebis, K.; Jones, M. W.; Haddleton, D. M.; Gibson, M. I. Thermoresponsive behaviour of poly[(oligo(ethyleneglycol methacrylate)]s and their protein conjugates: importance of concentration and solvent system. *Polym. Chem.* **2011**, *2* (4), 975−982.
(24) Pechar, M.; Pola, R.; Laga, R.; Braunova, A.; Filippov, S. K.; Bogomolova, A.; Bednarova, L.; Vanek, O.; Ulbrich, K. Coiled Coil Peptides and Polymer-Peptide Conjugates: Synthesis, Self-Assembly, Characterization and Potential in Drug Delivery Systems. *Biomacromolecules* **2014**, *15* (7), 2590−2599.
(25) Carlisle, R.; Choi, J.; Bazan-Peregrino, M.; Laga, R.; Subr, V.; Kostka, L.; Ulbrich, K.; Coussios, C. C.; Seymour, L. W. Enhanced Tumor Uptake and Penetration of Virotherapy Using Polymer Stealthing and Focused Ultrasound. *Jnci-J. Natl. Cancer I* **2013**, *105* (22), 1701−1710.
(26) Sirova, M.; Kabesova, M.; Kovar, L.; Etrych, T.; Strohalm, J.; Ulbrich, K.; Rihova, B. HPMA Copolymer-Bound Doxorubicin Induces Immunogenic Tumor Cell Death. *Curr. Med. Chem.* **2013**, *20* (38), 4815−4826.
(27) Etrych, T.; Mrkvan, T.; Chytil, P.; Konak, C.; Rihova, B.; Ulbrich, K. N-(2-hydroxypropyl)methacrylamide-based polymer conjugates with pH-controlled activation of doxorubicin. I. New synthesis, physicochemical characterization and preliminary biological evaluation. *J. Appl. Polym. Sci.* **2008**, *109* (5), 3050−3061.
(28) Ulbrich, K.; Subr, V.; Strohalm, J.; Plocova, D.; Jelinkova, M.; Rihova, B. Polymeric drugs based on conjugates of synthetic and natural macromolecules I. Synthesis and physico-chemical characterisation. *J. Controlled Release* **2000**, *64* (1−3), 63−79.
(29) Ulbrich, K.; Etrych, T.; Chytil, P.; Jelinkova, M.; Rihova, B. Antibody-targeted polymer-doxorubicin conjugates with pH-controlled activation. *J. Drug Target* **2004**, *12* (8), 477−489.
(30) Subr, V.; Ulbrich, K. Synthesis and properties of new N-(2-hydroxypropyl)-methacrylamide copolymers containing thiazolidine-2-thione reactive groups. *React. Funct. Polym.* **2006**, *66* (12), 1525−1538.
(31) Chytil, P.; Etrych, T.; Kriz, J.; Subr, V.; Ulbrich, K. N-(2-Hydroxypropyl)methacrylamide-based polymer conjugates with pH-controlled activation of doxorubicin for cell-specific or passive tumour targeting. Synthesis by RAFT polymerisation and physicochemical characterisation. *Eur. J. Pharm. Sci.* **2010**, *41* (3−4), 473−482.
(32) Etrych, T.; Subr, V.; Laga, R.; Rihova, B.; Ulbrich, K. Polymer conjugates of doxorubicin bound through an amide and hydrazone bond: Impact of the carrier structure onto synergistic action in the treatment of solid tumours. *Eur. J. Pharm. Sci.* **2014**, *58*, 1−12.
(33) Nakamura, H.; Etrych, T.; Chytil, P.; Ohkubo, M.; Fang, J.; Ulbrich, K.; Maeda, H. Two step mechanisms of tumor selective delivery of N-(2-hydroxypropyl) methacrylamide copolymer conjugated with pirarubicin via an acid-cleavable linkage. *J. Controlled Release* **2014**, *174*, 81−87.
(34) Hovorka, O.; St'astny, M.; Etrych, T.; Subr, V.; Strohalm, J.; Ulbrich, K.; Rihova, B. Differences in the intracellular fate of free and polymer-bound doxorubicin. *J. Controlled Release* **2002**, *80* (1−3), 101−117.
(35) Hovorka, O.; Subr, V.; Vetvicka, D.; Kovar, L.; Strohalm, J.; Strohalm, M.; Benda, A.; Hof, M.; Ulbrich, K.; Rihova, B. Spectral analysis of doxorubicin accumulation and the indirect quantification of

DOI: 10.1021/acs.biomac.5b00764
Biomacromolecules XXXX, XXX, XXX−XXX

its DNA intercalation. *Eur. J. Pharm. Biopharm.* **2010**, *76* (3), 514−524.
(36) Nakamura, H.; Etrych, T.; Chytil, P.; Ohkubo, M.; Fang, J.; Ulbrich, K.; Maeda, H. Two step mechanisms of tumor selective delivery of N-(2-hydroxypropyl) methacrylamide copolymer conjugated with pirarubicin via an acid-cleavable linkage (vol 174, pg 81, 2014). *J. Controlled Release* **2014**, *182*, 97−98.
(37) Weerasinghe, P.; Buja, L. M. Oncosis: An important non-apoptotic mode of cell death. *Exp. Mol. Pathol.* **2012**, *93* (3), 302−308.

DOI: 10.1021/acs.biomac.5b00764
Biomacromolecules XXXX, XXX, XXX−XXX